POLARIMETRIC ANALYSIS OF DE GERLACHE CRATER USING CHANDRAYAAN-2 DFSAR DATA.

Hamish Dsouza[1] and Shashi Kumar[1], [1]Indian Institute of Remote Sensing, ISRO (hamish.iirs@gmail.com)

Introduction: Considering the risk to human life and the high economic costs of human exploration missions to the Moon, remote sensing analysis of areas of interest are necessary to analyze the resource potential and the risk involved. The de Gerlache crater is an important site for human exploration of the Moon and has three of the thirteen candidate landing sites of the Artemis III mission. Permanently Shadowed Region (PSR) SP_883129_2691439 that lies within de Gerlache crater is invisible to optical sensors. The presence of craters from two different ages further adds to the complexity of this crater. Since radars are active sensors, Dual Frequency Synthetic Aperture Radar (DFSAR) on board Chandrayaan-2 can be used to analyze such PSRs.

DFSAR Data: DFSAR is the first L-band sensor outside the Earth with an objective to quantify water-ice in polar regions. With a slant resolution of 2-75m, this sensor can be used to generate high resolution maps of the Moon. The data can be used for characterization of the surface, estimation of dielectric constant and detection of presence of surface ice clusters.

de Gerlache crater: Proximity to PSR SP_883129_2691439 that may hold water-ice over 2.3% of its surface [1], a topographic high point with one of the most illuminated regions on South Pole and high Earth visibility [2] for communication, make the de Gerlache crater an important resource location. L-band data from Chandrayaan-2 DFSAR was used to analyze the polarimetric scattering behavior over the surface of this crater.

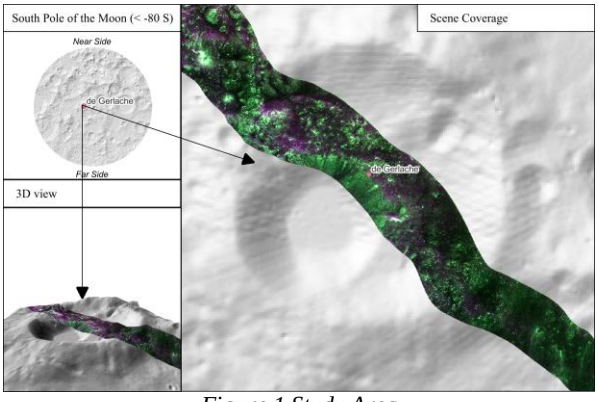

Figure 1 Study Area

Processing: DFSAR L-band Full-polarimetric dataset covering wall, rim, floor and ejecta was selected to analyze the different features. Scene ch2_sar_ncxl_20210212t023846346_d_sli_xx_fp_xx_d32 (product id: 212211) acquired at ~25.97° incidence angle over de Gerlache crater was used for analysis. The Single Look Complex Seleno tagged data was radiometrically calibrated to calculate the radar backscatter. Covariance (C3) and Coherency (T3) matrixes were generated. The derived matrices were multilooked (factor ~ 38) to generate square pixels and reduce speckle noise. Three regions each, on the wall, rim, floor and ejecta of the inner crater were observed. The matrices were decomposed using model based Freeman-Durden decomposition, Eigenvector based decompositions H/A/A decomposition and Model Free 3-component decomposition. H/A/A decomposition does not assume that the data follows a particular distribution and hence allows it to avoid certain model-based limitations. It uses a 3x3 coherency matrix to describe the scattering mechanism [3]. Freeman-Durden decomposition fits a physically based three-component scattering mechanism model to PolSAR observations without using any ground truth [4]. Model Free 3-Component decomposition: This method uses the 2-D and 3-D Barakat degree of polarization to decompose the coherency matrix to obtain scattering type parameter [5]

Results:

H/A/A decomposition: The entropy and mean α were analyzed for different classes.

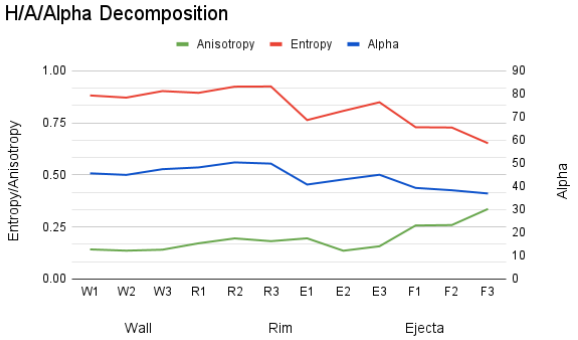

Figure 2 Entropy, Anisotropy and A from H/A/A Decomposition

At the walls of the crater, entropy was around 0.9, signifying an ensemble of scatters. The mean α was around 45°. The walls may be dominated by anisotropic scatterers. The rim of the inner crater had entropy above 0.9 and mean α 50°. This is typical of random anisotropic scatters tending towards noise. This could be due to the presence of close but loosely held particles on the rim. Entropy (0.76-0.8) and α (40°–43°) both reduce in the ejecta region. Anisotropy (0.19) shows a

slight increase in this region. On the floor of the outer crater, the entropy values are lesser than other regions but still higher than 0.7. Mean α reduces to 38°, showing the presence of surface scattering. The values of entropy (H) were high for all classes. Since most of the values were above 0.7, another factor Anisotropy was also considered. However, as seen in figure 2, the classes are not clearly distinguishable. Though H/A/A decomposition is widely used for polarimetric analysis, its applications for studying this crater using full polarimetric data is limited. H-A decomposition of compact-pol data from Chandrayaan-1 Mini-RF also shows high values of entropy in PSR thereby limiting the ability to distinguish between scattering mechanisms [6].

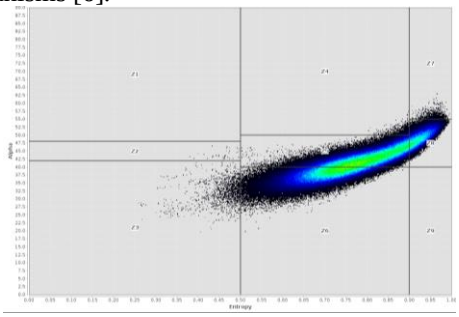

Figure 3 H-A Plane Plot

Freeman-Durden and Model Free 3 Component decomposition

The percentage of contributions of different scattering mechanisms according to Freeman-Durden (FD) decomposition and Model Free 3 Component (MF3C) decompositions were analyzed.

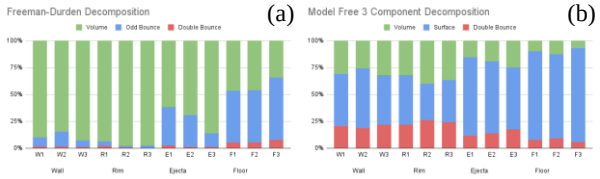

Figure 4 Distribution of scattering contribution according to (a) Freeman-Durden and (b) Model Free 3 Component decomposition

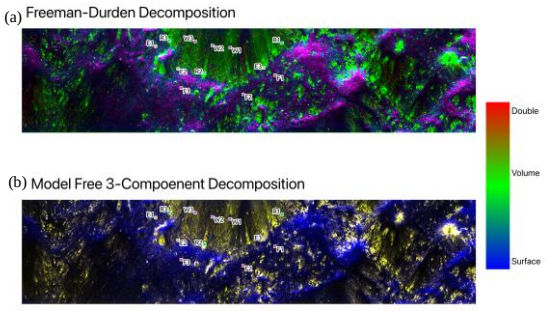

Figure 5 (a) Freeman Durden decomposed image (b) Model Free 3 Component decomposed image

On the walls of the crater, Freeman-Durden decomposition shows a dominance of Volume scattering while the Model Free 3 Component decomposition shows a dominance of Surface scattering. Double bounce is lower on the wall of the crater in both methods. On the rim of the crater, while the FD decomposition shows a dominance of volume scattering, the MF3C shows almost equal contributions from volume and surface scattering. However, both decompositions note the reduction of surface scattering behavior on the rim. The higher volume scattering could be due to presence of loosely held wavelength range regolith particles. The ejecta of the crater shows an increase in odd bounce and surface scattering. In MF3C, the surface scattering dominates in the ejecta region. This could be due to the penetration of L-band waves through the ejecta. However, the FD decomposition shows a dominance of volume scattering. Beyond the ejecta of the inner crater and on the floor of the outer crater. There is an increase in surface scattering for both decompositions. Some double bounce scattering is also seen. This could be due to boulders present on the floor.

Summary: Due to high entropy, the usability of H-α decomposition to analyze the crater was limited. Both model based Freeman Durden and Model Free 3 Component decomposition showed a dominance of surface and volume scattering, though differing in proportion. In the absence of optical data from the PSR under study, validating the decompositions is not possible. High resolution data of the thermal and mineralogical properties of the area can give further insights into its resource potential.

Acknowledgement: We acknowledge the use of data from the Chandrayaan-II, second lunar mission of the Indian Space Research Organisation (ISRO), archived at the Indian Space Science Data Centre (ISSDC)

References: [1] Kring D.A. et al. (2020) *LPI Contribution 2557*.[2] Mazarico,E., et al. (2011) *Icarus, 211* [3] Lee J.S and Pottier E. (2009) Polarimetric Radar Imaging [4]Freeman A. and Durden S.L *IEEE Trans.Geosci. Remote Sens 36(3).*[5]Dey S. et al. *IEEE Trans.Geosci. Remote Sens 59(5).* [6] *Saran S.et al.* (2015) *LPSC XLVI #1916*